

MEASURING FIBRE-FIBRE CONTACT IN 3D IMAGES OF FIBROUS MATERIALS

F. Malmberg¹, J. Lindblad¹, C. Östlund^{1,2}, K. M. Almgren² and E. K. Gamstedt^{2,3}

¹Centre for Image Analysis, Swedish University of Agricultural Sciences, Uppsala, Sweden

²STFI-Packforsk AB, Stockholm, Sweden

³KTH Fibre and Polymer Technology, Royal Institute of Technology, Stockholm, Sweden
{filip, joakim}@cb.slu.se, {catherine.ostlund, karin.almgren, kristofer.gamstedt}@stfi.se

ABSTRACT

The degree of fibre-fibre bonding plays a fundamental role in the mechanical properties of paper materials and fibre mats. In this work, a method for measuring the amount of fibre-fibre bonds in volume images of fibrous materials is presented. The method consists of two parts. First, fibre lumens are segmented using a watershed based method. This information is then used to identify fibre-fibre bonds in projections along the z -axis of the material. The method is tested on microtomography images of pulp-fibre composite materials, and is shown to successfully detect differences in the amount of fibre-fibre bonds between the samples.

1 INTRODUCTION

Mechanical properties, such as stiffness and strength, of paper and board are highly dependent on the amount and strength of fibre-fibre bonds. A common measure of the amount of fibre-fibre bonds is relative bonded area (RBA), defined as the ratio of bonded area to the total surface area of the fibres.

$$RBA = \frac{\text{Bonded fibre surface area}}{\text{Total fibre surface area}}$$

A measure of RBA does not give any information of the type or strength of the fibre-fibre bonds. The correlation between RBA and paper properties is nevertheless well established. Paper stiffness was studied by Page et al. [16] and van den Akker [8] and was found to be dependent on RBA of the sheet. Page [16] also developed a theory for paper strength, that links RBA to the strength of paper. Ingmanson and Thode [12] found that the strength of paper increases with increasing refining time. Their study also showed that the RBA increases with increasing refining time, suggesting that RBA is an important parameter affecting paper strength. Carlsson and Lindström [7] used a shear-lag approach for predicting the strength of paper and found that transition from fibre pull-out to fibre breakage strongly affects the paper strength and is highly dependent on the strength of fibre-fibre bonds and on RBA.

Mechanical properties are of great importance also for pulp-fibre composites, a relatively new use of pulp fibres, where they are used as reinforcement in a polymeric matrix. This type of material could be suitable for e.g. packaging and as panels for automotive applications. Other types of natural reinforcing fibres are flax, hemp and jute. Today several natural-fibre composite products are available on the market but the potential of pulp fibres as reinforcement has not yet been fully explored. Depending on the adhesion between the polymeric matrix and the



Figure 1: Surface rendering of fibres in a pulp-fibre composite material imaged in 3D using X-ray microtomography. The average cross-sectional diameter of the fibres is approximately $30 \mu\text{m}$.

fibres and the wettability of the fibres, fibre-fibre bonds could be of importance for mechanical properties also of pulp-fibre composites.

Recent advances in imaging technology have made it possible to capture three-dimensional (3D) images of pulp fibre based materials with high resolution [1]. Analysis of such images can provide very detailed knowledge about the microstructure of the material, which in turn controls the mechanical properties. A computer generated image of fibre surfaces extracted from a high resolution 3D image of a pulp-fibre composite material is shown in Figure 1.

We will make a distinction between *fibre-fibre bonds* and *fibre contact*. The terms *fibre-fibre bond* or *bonding* are used to denote stress-transferring bonds, briefly described in [11], and bonded area is the area in which these types of bonds are present. The term *fibre contact* is used to describe contact between fibres studied with image analysis tools. Fibres in contact are not necessarily bonded and the contact area may hence be larger than the bonded area.

Here, a method for measuring the amount of fibre-fibre contact in binary 3D images of fibrous materials is presented. The method is based on segmenting all non-fibre regions of the image into lumen and background. This information is then used to identify fibre-fibre contacts of uncollapsed fibres. The method is tested on samples of pulp-fibre composite material, imaged using X-ray microtomography (μCT).

2 BACKGROUND

2.1 Existing methods for measuring RBA

Various direct and indirect methods have been suggested to estimate RBA. A commonly used measure of RBA is determined through comparison of light scatter in the studied sample and in an unbonded reference sheet [12, 20, 13, 14]. It is, however, difficult to manufacture reference sheets where the degree of fibre-fibre bonding is the only parameter that varies. Surfaces inside lumens and microcracks in the fibre wall will be identified as free surfaces, which could make the method uncertain.

The absorption of nitrogen gas has been suggested to give a more accurate measure of RBA [9, 10] due to the smallness of nitrogen molecules, but the amount of collapsed fibres will affect the result also when using this technique [21].

The methods discussed above are indirect but are used to approximate the RBA in paper.

None of them can however be used to study fibre contact in pulp-fibre composites, since the optical properties of the polymeric matrix affects light scattering and gas absorption is hindered. The development of new tools for the study of fiber contact in pulp-fibre composites is therefore important for the development of this type of material.

2.2 Measuring fibre-fibre contact using image analysis

The most direct way to measure fibre-fibre contacts in digital 3D images would be to segment all individual fibres. Image segmentation means assigning to each image element a label that indicates to which object it belongs. Given a complete segmentation of all individual fibres, measuring the area of the fibres and the area of fibre-fibre intersections is trivial. Yang et al. [24] measured fibre-fibre contact by manually delineating fibres in cross-sections of paper samples. Manual delineation of large numbers of fibres is highly unpractical, so more automated segmentation methods are needed for this approach. Automatic segmentation of individual fibres is, however, a very difficult task. This is due both to the fact that the fibre network can be very dense and complicated, and that the fibres themselves can be so damaged and deformed during the manufacturing process that it is hard to find common characteristics for the shape of a fibre. In particular, the presence of shives and processing-induced fibre fragments in thermomechanical pulp complicates quantitative image analysis. Several automatic methods for segmenting individual fibres have been proposed in the literature, see e.g. [2, 4, 15, 23], but none of these seem to give results that are accurate and complete enough for our purposes. In this work an image analysis method for measuring fibre-fibre contact, that does not require segmentation of individual fibres, is used instead. The idea is that segmenting all non-fibre voxels into lumens and background is an easier task than segmenting individual fibres, yet the information from such a segmentation can be used to identify fibre-fibre contacts. The proposed method is conceptually similar to the light scattering method in that we identify phase changes along rays through the material. However, in contrast to the light scattering method, we can use the information from the lumen segmentation to handle surfaces inside lumens correctly.

2.3 Previous work on lumen segmentation

A number of methods for segmenting lumens in 3D images of fibrous materials exist in the literature. Lux et al. [15] use morphological dilation to close small holes in the fibre-walls, and thus separate the lumens from the background. All isolated regions are then filled, and an erosion is performed to undo the dilation. This approach is based on the assumption that lumens can be modeled as regions that are isolated from the background by fibre material, with the exception of small holes in the fibre wall. Some holes or pits occur naturally in the fibre wall and are used to transport sap and water between adjacent fibres. These include, e.g., narrow cross-field pits and circular bordered pits in pine, and rectangular window pits in spruce [18]. Additional holes and breaks may be caused by damage to the fibres during the pulping process and errors in the pre-processing and binarization of the images. The result of this method is an image where the lumens are filled, i.e. there is no distinction between the fibre wall and the lumen in the result. In this case, a 3D image that contains only the lumens can not be produced by taking the difference between the original binary image and the filled image, since the morphological operations may change the shape of the fibre wall. A similar approach is used in [23], where morphological closing is used to close the holes in the fibre wall. Since the shapes of the isolated regions are changed by the closing operation, region growing

is applied as a post-processing step to restore the shape of the segmented lumens. This method segments individual lumen, i.e. each lumen gets a unique label in the resulting image. Using morphological operations to close holes in the fibre walls means setting a global threshold on the allowed size of the holes. The lumen segmentation method presented in this work uses a similar assumption about the characteristics of a lumen as the two methods described above, i.e. lumens can be modeled as partially isolated regions. However, instead of using morphological operations to isolate the lumens, the method is based on watershed segmentation [22]. This allows the threshold on the size of the fibre wall holes to be adjusted locally. The size of a hole in a fibre wall may, e.g., be compared to the size of the interior region to determine if the region is a lumen. Other features of the regions and the interfaces between them can also be incorporated into this decision. The watershed method, in contrast to methods based on morphological operations, operates directly on the original fibre shapes. Thus, no post-processing is required to ensure that the shapes of the segmented lumens match the shapes of the fibres.

3 METHOD

The proposed method for measuring the amount of fibre-fibre contact in a binary 3D image of a fibrous material consists of two parts. First all non-fibre voxels are segmented into lumens and background, using a method based on watershed segmentation. Fibre-fibre contacts are then identified in projections along the z -axis of an image where each voxel is labeled as either fibre, lumen, or background.

3.1 Lumen segmentation

The first step in the lumen segmentation method is to apply a distance transform (DT) to the background of the image, followed by a watershed segmentation of the inverse image of the DT. Our implementation of the method uses the Euclidean DT, but other distance definitions could be used as well. For an introduction to distance transforms, see e.g. [5]. The watershed region that contains the largest distance value, i.e. the largest open space, is assumed to represent the background. Since the watershed algorithm starts labeling small values first, and small values in the inverted DT corresponds to large distances, the largest open space is simply the first labeled region. Our strategy is to merge other regions with the background until only the regions representing the lumens remain. Various features of the regions are used to determine which regions should be merged. The result is a binary volume where voxels that belong to a lumen have label 1 and all other voxels have label 0. The first criterion used for merging regions is the concept of throat-size [17]. If the maximum distance value on the border surface between two regions is larger than a threshold t_1 , then the regions are merged. All regions that are not part of the background after this merging step are considered to be lumen candidates. At this stage there are many false "lumens", so some additional steps are needed. The second criterion is that the area of the interface between a lumen and the background should be small compared to the surface area of the lumen. This assumption is, however, often violated because of the oversegmentation inherent in the watershed method. To reduce oversegmentation, an intermediate merging step is applied to the lumen candidates. To determine which regions should be merged, the concept of *relative shared area* (RSA) is introduced. The RSA between two regions r_1 and r_2 is defined as the ratio between the area of the interface of the regions and the surface area of the smaller region:

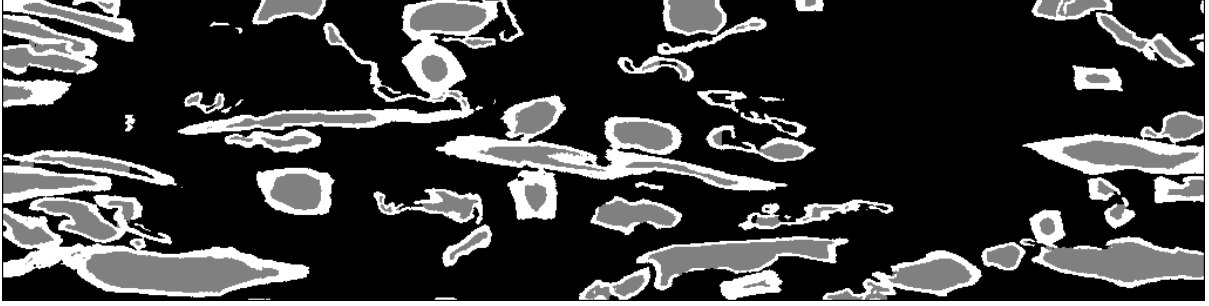


Figure 2: A 2D slice from the result of the proposed lumen segmentation method. White pixels represent fibre material, black pixels are background and grey pixels are the segmented lumens. The average diameter of the fibres oriented out of plane is approximately $30 \mu\text{m}$.

$$RSA(r_1, r_2) = \frac{\text{area of the interface between } r_1 \text{ and } r_2}{\min\{\text{surface area of } r_1, \text{ surface area of } r_2\}}$$

The surface area of a region is, in this case, defined as the number of voxels in the region that are 6-connected to a voxel that does not belong to the region. The area of the interface between two regions is defined as the number of voxels in the region with the smaller surface area that are 6-connected to the region with the larger surface area. For each lumen candidate region, the RSA between the region and all its adjacent lumen candidate regions is computed. If the RSA of two lumen candidate regions is larger than a threshold t_2 , the regions are merged. Finally, the RSA between each region and the background is computed. If the RSA value of a region is larger than a threshold t_3 , that region is merged with the background.

An example of the results of this method is shown in Figure 2. Pseudocode for the method is listed in Appendix 1.

3.2 Identifying fibre-fibre contacts

The result of the lumen segmentation is used to create a new image, where each voxel is labeled as either background, fibre, or lumen. See Figure 2. Fibre-fibre contacts are then identified by traversing rays along the z -axis of this image. Each time two separate lumen regions connected by only fibre material along a ray are encountered, a contact is considered found. It is assumed that most fibre-fibre intersections are approximately perpendicular to the z -axis of the image, and therefore only rays along the z -axis are considered. Other directions may also be used for samples where this assumption does not hold. The total contact area, $A_{contact}$, is defined as the number of identified contacts. The total surface area, A_{total} , is measured in a similar way by counting the number of times the data changes from background to material along each ray, i.e. from matrix to fibre or vice versa. Since only the outside area of the fibres should be included in the area measure, i.e. not the surface area of the lumens, the voxels identified as lumens are also considered to be part of the fibre. It should be noted that this definition of area is equivalent to projecting all area elements onto the x,y -plane before summing them. This makes sense in our case, because the exact location of the contacts in the z -direction are not known. Finally, the *relative contact area* (RCA) is achieved by dividing $A_{contact}$ by A_{total} :

$$RCA = \frac{A_{contact}}{A_{total}}$$

Table 1: Parameters for lumen segmentation

Sample	t1	t2	t3
C1	7	0.4	0.08
C2	15	0.4	0.13
C3	7	0.4	0.13

Table 2: Description of processing of the composite materials

Composite	Description of paper sheet	Degree of fibre-fibre bonding
C1	reference, wet pressure: 0 bar	highest
C2	isopropanol, wet pressure: 2 x 0.5 bar	high
C3	isopropanol, wet pressure: 0 bar	lower

4 EXPERIMENTAL PROCEDURES

The method was tested on composite materials where the fibres are immobilized by a surrounding matrix. The composite samples used were made through impregnation of paper sheets with a thermoset polymeric matrix (epoxy vinyl ester). Different levels of wet pressure and solvent exchange was used to vary the amount of fibre-fibre bonds in the paper sheets. The isopropanol solvent reduces the amount of fibre-fibre bonds, while pressing increases the amount of bonds. Composites were produced from the different types of paper sheets using a resin transfer moulding technique, where high pressure at the resin inlet and vacuum suction at the outlet is used to impregnate the paper sheets with the viscous resin, which is subsequently cured to form a solid composite plate.

Light scattering experiments to estimate the total fibre area of sheets manufactured after solvent exchange show unexpectedly high fibre areas, which can be explained by fibre shrinkage enhanced by solvent exchange [12]. These effects are disregarded in this study, since focus is placed on the relative effect of fibre-fibre bonding vs. fibre-matrix interface on mechanical properties of composites.

Processing conditions of the different samples, and a rough estimate of the degree of fibre-fibre bonding in the paper sheet used to make the composites, are shown in Table 2. The unconsolidated paper sheets have lower tensile stiffness, in-plane strength and z-strength than the consolidated sheets, indicating a lower degree of fibre-fibre bonding.

The samples were imaged using X-ray microtomography at beamline ID19 at the European Synchrotron Radiation Facility (ESRF) in Grenoble, France. The tomograph gives 3D images of the samples with high resolution. The resolution of a volume element, voxel, in the images is $0.7\mu\text{m} \times 0.7\mu\text{m} \times 0.7\mu\text{m}$ and the size of each volume is about $2048 \times 2048 \times 1280$ voxels.

To measure the amount of fibre-fibre contact in the images, they must first be segmented into fibre and background. X-ray microtomography, as well as any other imaging modality, gives rise to artifacts and noise that has to be removed. In our case, ring artifacts present were reduced using a method by Axelsson et al. [3]. Image noise was reduced using a 3D edge preserving filtering method [19]. The volumes could then be segmented into fibre and background using hysteresis thresholding [6]. The different steps of preprocessing are shown in Figure 4. Lumen segmentation was then performed using the parameters shown in Table 1. The parameters were determined by visual inspection of the segmentation results.

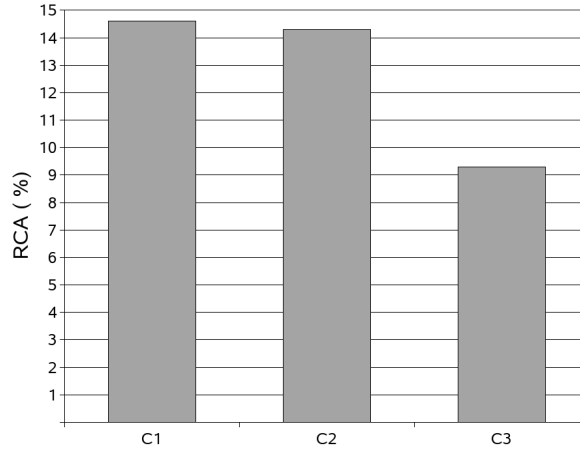


Figure 3: Relative contact areas measured using the proposed method on the three composite material samples in the experiment.

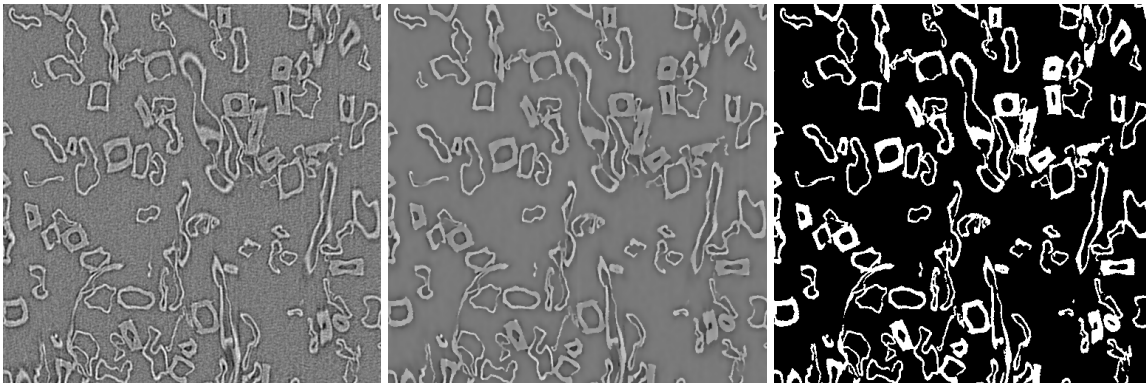


Figure 4: Segmenting the volume into fibre and background. a) A slice of the original volume after ring-artifact reduction. b) The same slice after edge preserving filtering. c) The same slice after hysteresis-thresholding.

5 RESULTS

Resulting measurements for the samples in the experiment are shown in Figure 3. The results agree with the expected results as described in Table 2, i.e. sample C1 has the highest amount of fibre contact, sample C2 has a slightly lower degree of fibre contact, and sample C3 has the lowest degree of fibre contacts. These values are slightly lower than earlier estimates where indirect methods were used [12].

6 CONCLUSIONS

We have proposed an image analysis method for measuring fibre-fibre contact in 3D images of fibrous materials. The method is conceptually similar to the light scattering method, but has the advantage that surfaces inside lumens are handled correctly. In contrast to previous, indirect, methods for measuring RBA and fibre contact area, the proposed method also works for composite materials. In the performed experiments, the proposed method correctly identified differences in the amount of fibre-fibre contacts between a number of samples. The method is based on the assumption that all fibres have a detectable lumen, which is not always the case,

since lumens may be collapsed. The lumens are also assumed to be convex with respect to the direction of the rays, i.e. a ray should not pass through the same fibre wall more than twice. This holds for most of the fibres in the studied images, and in the few cases where concavities occur the error introduced is negligible. The accuracy of the measurements depends on the quality of the lumen segmentation. Since no ground-truth data exists for the lumen segmentation, it is hard to quantitatively access the quality of the segmentation. However, visual inspection indicates that if proper parameters are used, good results can be achieved. How the parameters of the lumen segmentation method should be set depends on the size and amount of holes in the fibre walls, as well as the overall density of the volume. Suitable parameters are harder to find for very dense volumes, since the assumption that all isolated regions are lumens does not hold for such volumes. The lumen segmentation method presented in this paper differs from previous methods in that it uses the watershed method instead of morphological operations. This allows the use of local features to determine if a region belongs to a lumen. The features used in this paper are throat size and relative shared area, but other features could easily be incorporated into the method, i.e. if additional information about the fibre network is available.

ACKNOWLEDGEMENT

The European Synchrotron Radiation Facility (ESRF) in Grenoble is gratefully acknowledged for the 3D image data, acquired during the Long Term project ME-704, that were used in this study. Prof. Gunilla Borgefors at the Centre for Image Analysis, Swedish University of Agricultural Sciences, Uppsala, Sweden, is acknowledged for her scientific support.

References

- [1] C. Antoine, P. Nygård, Ø. W. Gregersen, R. Holmstad, T. Weitkamp, and C. Rau. 3d images of paper obtained by phase-contrast x-ray microtomography: image quality and binarization. *Nuclear Instruments and Methods in Physics Research Section A: Accelerators, Spectrometers, Detectors and Associated Equipment*, 490(1-2):392, 2002.
- [2] M. Aronsson. *On 3D fibre measurements of digitized paper*. PhD thesis, Swedish University of Agricultural Sciences, Uppsala, Sweden, 2003.
- [3] M. Axelsson, S. Svensson, and G. Borgefors. Reduction of ring artifacts in high resolution X-ray microtomography images. In F. et al., editor, *Proceedings of DAGM*, volume LNCS 4174, page 61, 2006.
- [4] J. Bache-Wiig and P. Henden. Individual fiber segmentation of three dimensional microtomograms of paper and fiber-reinforced composite materials. Master's thesis, Norwegian University of Science and Technology, 2005.
- [5] G. Borgefors. Distance transformations in digital images. *Computer Vision, Graphics, and Image Processing*, 34(3):344, 1986.
- [6] J. F. Canny. A computational approach to edge detection. *IEEE Transactions on Pattern Analysis and Machine Intelligence*, 8(6):679, 1986.
- [7] L. Carlsson and T. Lindström. A shear-lag approach to the tensile strength of paper. *Compos. Sci. Technol.*, 65(7-8):183, 2005.
- [8] J. V. DeAkker. Structure and tensile characteristics of paper. *Tappi*, 53(3):388, 1970.
- [9] W. Haselton. Gas adsorption of wood, pulp and paper. 1. the low temperature adsorption of nitrogen, butane and carbon dioxide by spruce wood and its components. *Tappi*, 37(9):404, 1954.

- [10] W. Haselton. Gas adsorption of wood, pulp and paper. 2. the application of gas adsorption techniques to the study of the area and structure of pulps and the unbonded and bonded area of paper. *Tappi*, 38(12):716, 1955.
- [11] H. Higgins. Sticking together - how interfibre cohesion works. *Appita J*, 55(3):187, 2002.
- [12] W. Ingmanson and E. Thode. Factors contributing to the strength of a sheet of paper. *Tappi*, 42(1):83, 1959.
- [13] F. Keeney. Physical properties of slash pine semi-chemical kraft pulp and of its fully chlorited component. *Tappi*, 35(12):555, 1952.
- [14] P. Luner, A. Kärnä, and C. Donofrio. Studies in interfiber bonding of paper, the use of optically bonded areas with high yield pulps. *Tappi*, 44(6):409, 1961.
- [15] J. Lux, C. Delisée, and X. Thibault. 3D characterization of wood based fibrous materials: an application. *Image Analysis and Stereology*, 25:23, 2006.
- [16] D. Page, R. Seth, and J. DeGrace. The elastic modulus of paper. *Tappi*, 62(9):99, 1979.
- [17] I. Sintorn, S. Svensson, M. Axelsson, and G. Borgfors. Segmentation of individual pores in 3D paper images. *Nordic Pulp and Paper Research Journal*, 20(3), 2005.
- [18] J. Sirviö and P. Kärenlampi. Pits as natural irregularities in softwood fibers. *Wood Fiber Sci.*, 30(1):27, 1998.
- [19] S. Smith and J. Brady. SUSAN- a new approach to low level image processing. *Int. Journal of Computer Vision*, 23(1):45, 1997.
- [20] J. Swanson and J. Anthony. Fiber surface area and bonded area. *Tappi*, 42(12):986, 1959.
- [21] T. Uesaka, E. Rtulainen, L. Paavilainen, E. Mark, and D. Keller. *Handbook of Physical testing*, page 873. Marcel Dekker Inc., New York, 2002.
- [22] L. Vincent and P. Soile. Watersheds in digital spaces: An efficient algorithm based on immersion simulations. *IEEE Transactions on Pattern Analysis and Machine Intelligence*, 13(6):583, 1991.
- [23] T. Walther, K. Terzic, T. Donath, H. Meine, F. Beckmann, and H. Thoemen. Microstructural analysis of lignocellulosic fiber networks. In Bonse and Ulrich, editors, *Developments in X-Ray Tomography V. Proceedings of the SPIE.*, volume 6318, Aug. 2006.
- [24] C. Yang, A. Eusufzai, R. Sankar, R. Mark, and R. P. Jr. Measurements of geometrical parameters of fiber networks. part 1. bonded surfaces, aspect ratios, fiber moments of inertia, bonding state probabilities. *Svensk Papperstidning*, 13(81):426, 1978.

APPENDIX 1

Pseudocode for the lumen segmentation algorithm.

Algorithm 1 Lumen segmentation

Input: A binary image i of the fibre network. Threshold values t_1 , t_2 and t_3

Output: A binary image $lumen$ containing the segmentation result.

```
1: Compute a distance transform  $dt$  on the background of  $i$ .
2: Compute the watershed segmentation  $ws$  of the inverse image of  $dt$ .
3: for all regions  $r \in ws$  do
4:   for all regions  $r_a$  adjacent to  $r$  do
5:     if the throatsize between  $r$  and  $r_a$  is smaller than  $t_1$  then
6:       Merge  $r$  and  $r_a$  and assign the label  $\min\{label(r), label(r_a)\}$  to the result.
7:     end if
8:   end for
9: end for
10:  $bglabel = \min_{r \in ws} label(r)$ 
11:  $bg \leftarrow \{r \in ws \mid label(r) = bglabel\}$ 
12: for all regions  $r \in \{ws \setminus bg\}$  do
13:   for all regions  $r_a \in \{ws \setminus bg\}$  adjacent to  $r$  do
14:     if  $RSA(r, r_a)$  is larger than  $t_2$  then
15:       Merge  $r$  and  $r_a$  and assign the label  $\min\{label(r), label(r_a)\}$  to the result.
16:     end if
17:   end for
18: end for
19: for all regions  $r \in \{ws \setminus bg\}$  adjacent to  $bg$  do
20:   if  $RSA(r, bg)$  is larger than  $t_2$  then
21:     Merge  $r$  and  $bg$  and assign the label  $bglabel$  to the result
22:   end if
23: end for
24:  $lumen \leftarrow \{r \in ws \mid label(r) \neq bglabel\}$ 
```
